

Preferential Nucleation of Metallic Clusters on a Nanotemplate: Co on Oxygen-Faceted Re(12 $\bar{3}$ 1)

Meral Reyhan · Hao Wang · Theodore E. Madey

Received: 9 September 2008 / Accepted: 21 September 2008 / Published online: 4 February 2009
© Springer Science+Business Media, LLC 2009

Abstract Preferential nucleation of cobalt nanoclusters at specific sites on oxidized faceted Re(12 $\bar{3}$ 1) is investigated by means of Auger electron spectroscopy (AES), low energy electron diffraction (LEED), and scanning tunneling microscopy (STM). An oxygen terminated nanofaceted Re surface containing ridges and valleys is used as the nanotemplate in this study. Deposition of cobalt onto this surface, followed by annealing to ~ 800 K, results in preferential cobalt nanocluster nucleation and growth within the valleys of the nanofaceted surface. Decreasing the nanofacet width, cobalt coverage, and annealing temperature lead to the same preferential cobalt nanocluster self assembly, an increase in nanocluster density, and a decrease in nanocluster volume. The preferential nucleation and growth observed for Co nanoclusters on faceted Re makes this a model system for future studies of different substrates and metallic overlayers more relevant to catalytic reactions.

Keywords Nanotemplate · Rhenium · Cobalt · Oxide · Facet · Nanocluster · Scanning tunneling microscopy

1 Introduction

Catalytic activity, expressed as product molecules per site per second, has been a primary focus of research in heterogeneous catalysis. It has been suggested that selectivity,

producing a specific reaction pathway out of several thermodynamic possibilities, should be the main focus of catalysis research for the twenty-first century [1, 2]. Several studies have shown that nanoparticle shape and size affect reaction rate and selectivity of supported metallic catalysts [1, 3–6]. Difficulties arise, however, in the production of supported catalytic nanoparticles with relatively narrow size distributions which can be varied in size and shape systematically; various growth procedures have been proposed and many show promise [2, 7–15]. A particular challenge is to develop a technique for self assembly of metal nanoclusters that are spatially separated and have a relatively narrow size distribution. We address this topic in the present paper.

Here we present an investigation of preferential Co nanocluster nucleation on a faceted self-assembled nanotemplated substrate, Re(12 $\bar{3}$ 1); we report how the oxygen-covered nanotemplate (Re) affects the nucleation and growth of a sample vapor-deposited metal (Co). In previous measurements, the procedure for formation of oxygen-induced nanofacets on Re(12 $\bar{3}$ 1) has been described [16]. Scanning tunneling microscopy, low energy electron diffraction (LEED), and Auger electron spectroscopy (AES) are used to characterize this system, providing direct insight into the nucleation and growth of the Co nanoclusters. By dosing Co onto a nanofaceted Re(12 $\bar{3}$ 1) surface, followed by annealing the surface, Co nanoclusters are observed to nucleate preferentially within the valleys of the faceted substrate.

2 Experimental

All experiments are performed in an ultra high vacuum (UHV) chamber with a base pressure about 1×10^{-10} Torr.

M. Reyhan · H. Wang · T. E. Madey (✉)
Department of Physics and Astronomy and Laboratory
for Surface Modification Rutgers, The State University
of New Jersey, Piscataway, NJ 08854, USA
e-mail: madey@physics.rutgers.edu

This chamber contains apparatus for Auger electron spectroscopy assembly, LEED optics, a quadrupole mass spectrometer, and a McAllister scanning tunneling microscope (STM). A $\text{Re}(12\bar{3}1)$ single crystal with a purity of 99.99%, approximately 10 mm in diameter and 1.5 mm thick, and cut within 0.5° of the $(12\bar{3}1)$ direction is used in this study. Oxygen is dosed onto the Re surface at room temperature by backfilling the chamber and pressures are measured using an uncalibrated Bayard–Alpert ionization gauge. The sample temperature is monitored using an infrared pyrometer. The Re crystal is cleaned by flash heating in vacuum to temperatures above 2,000 K and by cycles of e-beam heating in oxygen ($\sim 1 \times 10^{-7}$ Torr); cleanliness is verified using AES. All STM measurements are made with sample bias between 0.5 and 1.5 V and a tunneling current between 0.6 and 1 nA. The X, Y, and Z dimensions of the STM scan range are calibrated using atomically resolved STM images of $\text{S}(4 \times 4)/\text{W}(111)$ reconstruction and measurements of the tilt angle between the (211) and (111) planes on faceted $\text{O}/\text{W}(111)$ [17, 18]. The relative oxygen and cobalt coverages are determined from measurements of O/Re or Co/Re Auger peak height ratio as a function of dosing time at room temperature. The oxygen dose is expressed in units of Langmuir, L, $1 \text{ L} = 1 \times 10^{-6} \text{ Torr s} = 1.33 \times 10^{-4} \text{ Pa s}$. The cobalt dose is expressed in units of monolayers, ML, $1 \text{ ML} = 1 \times 10^{15} \text{ atoms/cm}^2$. Cobalt is dosed by a metal evaporator at a rate of approximately 0.20 ML/min.

3 Results and Discussion

An oxygen pressure of $\sim 1 \times 10^{-7}$ Torr was established in the vacuum chamber while the Re sample was heated to a temperature greater than 2,000 K; upon cooling in oxygen, a faceted surface with two facets $(01\bar{1}0)$ and $(11\bar{2}1)$ was observed using LEED [16]. STM measurements confirmed that these two facets form ridges longer than 350 nm; the average width of the ridges (peak to peak ridge distance) was approximately 20 nm and the average ridge height (peak to valley height) was approximately 2.8 nm. To minimize the extent of direct cobalt–rhenium interaction, the faceted surface was dosed with another 10 L of oxygen at 300 K before Co deposition to ensure that the surface is saturated with oxygen [16]. About 3.0 ML of Co was deposited and AES and LEED measurements were performed again to confirm the cobalt coverage and that the facets still remained. Then the $\text{Co}/\text{O}/\text{Re}(12\bar{3}1)$ faceted surface was annealed to approximately 800 K for 3 min; annealing the surface gave the cobalt the mobility needed to form the nanoclusters seen in Fig. 1.

Figure 1 shows that the Co nanoclusters nucleate preferentially in the troughs, or valleys. Cluster size needs to be

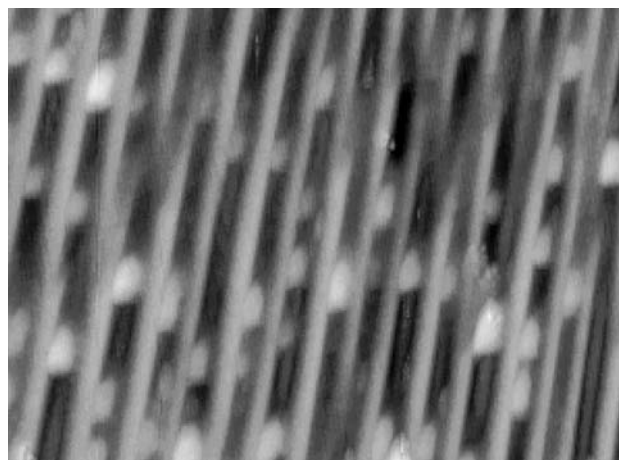


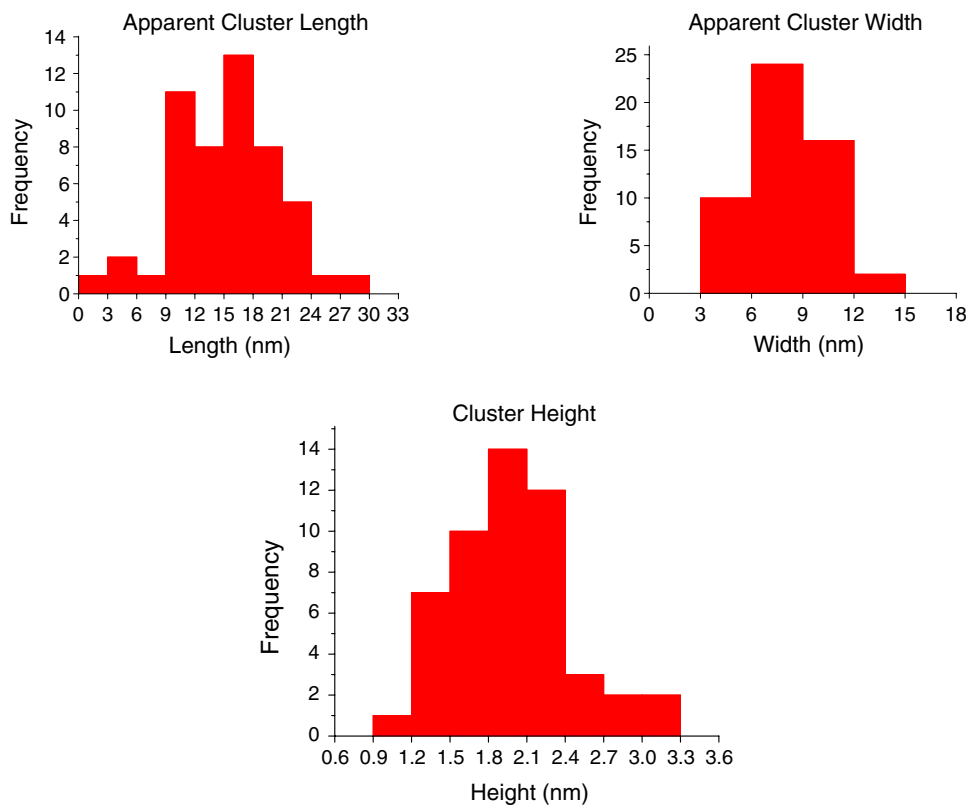
Fig. 1 After annealing the cobalt-covered faceted Re surface, preferential nucleation of cobalt nanoclusters in the facet valleys is clear from this $260 \times 170 \text{ nm}$ STM image. Approximately 3.0 ML of Co was dosed and the surface was annealed to $T \sim 800 \text{ K}$

corrected for the STM tip radius, which was determined to be approximately 1 nm based on “rounding” of the peaks of the ridges in Fig. 1. Taking into account the convolution of the STM tip radius and the nanocluster length and width, a simple geometric model [19] is utilized in conjunction with the mean values of the histograms, Fig. 2, to derive the corrected Co nanoclusters’ mean length of $14 \pm 4.0 \text{ nm}$, mean width of $6.4 \pm 2 \text{ nm}$, and mean height of $2.0 \pm 0.3 \text{ nm}$. The Co nanoclusters within the valleys of the faceted surface are approximately the same height as the ridges.

The two-dimensional Co cluster density is $810/\mu\text{m}^2$ (clusters per surface area). Since the clusters are elongated, the cluster shape is assumed to be ellipsoidal instead of spherical. It is also assumed that approximately 60% of the ellipsoidal volume corresponds to the actual nanocluster volume; this compensates for partial “wetting” of the faceted substrate by the nanoclusters. The volumes of the clusters are calculated individually using their respective length, width and height as the ellipsoidal axial parameters, from which the mean volume of a single cluster is determined as 58 nm^3 or 5.2×10^3 atoms. The fraction of Co incorporated in the clusters is approximately 0.42 ML or 14% of the total cobalt; the remaining Co is believed to cover the surface as a film.

In order to show that nanocluster size can be varied, other experiments were performed. The parameters changed in an attempt to control cluster size were facet width, cobalt coverage, and annealing temperature. By reducing the facet width (controlled by oxygen pressure and annealing temperature), the width of the nanoclusters was reduced as well. Decreasing the cobalt coverage reduced the volume of the nanoclusters.

Fig. 2 Histograms of Co nanocluster length, width, and height from the 3.0 ML of Co dosing experiment. The apparent or uncorrected length and width of the nanoclusters have mean values of 16 and 8.4 nm, respectively. These mean values are corrected with respect to the approximate STM tip radius and have mean values of 14 and 6.4 nm, respectively. The height is not affected by the STM tip radius in these measurements



A faceted O/Re($12\bar{3}1$) surface was generated, for which the average ridge width and height were approximately 10 and 1.5 nm, respectively, based on STM measurements. The surface was dosed with 1.6 ML of Co and AES and LEED measurements were performed again to confirm the cobalt coverage and faceting. The Co/O/Re($12\bar{3}1$) faceted surface was then annealed to a temperature less than 680 K for 3 min.

The resultant Co nanoclusters, visible in Fig. 3, have a corrected [19] mean length of 4.7 ± 1.2 nm, a mean width of 4.4 ± 1.2 nm, and a mean height of 2.5 ± 0.2 nm. Again, the Co nanoclusters remain within the valleys of the faceted surface and are taller than the height of the facets. The two-dimensional cluster density calculated as the number of clusters per surface area is $1,240/\mu\text{m}^2$. The approximate cluster volume, calculated as described above, is 20 nm^3 or 1.8×10^3 atoms. This shows an increase in cluster density and a decrease in volume in comparison with the 3.0 ML cobalt coverage experiment. The fraction of Co incorporated in the clusters is approximately 0.22 ML or 14% of the total cobalt.

To compare the narrow size dispersion of Co clusters in our study with other studies of metal clusters grown on oxide surfaces, we can compare dispersion parameters simply defined as the standard deviations of cluster dimensions divided by their respective mean values. The lateral dispersion parameters of Co clusters in our study are

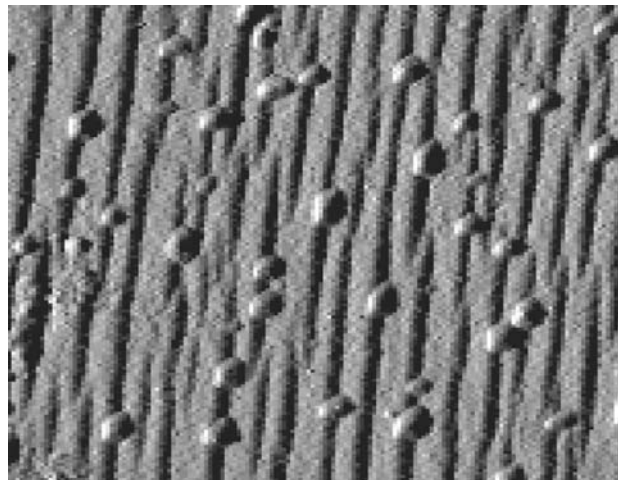


Fig. 3 This 130×140 nm STM image shows a reduction in facet size as well as Co nanocluster size in comparison; unlike Fig. 1, this is an x -slope (derivative) image. Approximately 1.6 ML of Co was dosed and the surface was annealed to $T \sim 680$ K prior to measurement

between 0.25 and 0.3, and the height dispersion parameter is less than 0.15. These parameters are close to those found in Ni clusters grown on $\text{TiO}_2(110)$ [20], Cu clusters on $\text{TiO}_2(110)-(1 \times 2)$ [21], Pd, Co or Rh clusters on Al_2O_3 films grown on $\text{NiAl}(110)$ [22], Fe on Al_2O_3 films grown on $\text{Ni}_3\text{Al}(111)$ [23], and Co on Al_2O_3 films grown on $\text{CoAl}(100)$ [24]. However, most of those studies did not

utilize any template to guide the cluster growth; the narrow cluster size dispersions could only be attained at 300–400 K due to the slow rate of atom diffusion, which may limit their potential use as supported model catalysts. In contrast, the narrow size dispersion of Co clusters found in our study is also affected by the uniform width distribution of the ridge template and can be realized upon annealing at temperatures as high as 800 K. The template assisted growth of metal clusters with narrow size distribution upon annealing at high temperatures can also be found in a recent study of Au clusters grown on TiO_x templates on Pt(111) [25].

Additional experiments were performed to confirm preferential nucleation and variability of cobalt nanocluster characteristics. The results from these experiments showed that decreased nanofacet width, cobalt coverage, and annealing temperature led to a decrease in nanocluster volume, and an increase in nanocluster density; in all cases nanoclusters preferentially nucleated in the nanofacet valleys. The amount of Co contained in the nanoclusters was determined as a function of cluster density and cluster volume; the results are consistent with Stranski–Krastanov (layer + island) growth as a result of the annealing process. In a recent study of Co nucleation and growth on a faceted Pt/W(111) surface, similar evidence for the formation of 3-D Co clusters correlated to the faceted Pt/W pyramids was reported, based on grazing incidence small angle X-ray scattering measurements (GISAXS) at the European Synchrotron Radiation Facility (ESRF) [26].

The precise nature of the nucleation sites and the reason for preferential nucleation of Co in the valleys has yet to be determined. However, for a cluster containing a given number of atoms, the largest fraction of interface atoms is expected for the valley sites. That is, the most effective surface wetting of Co on O/Re and the greatest surface area for Co–O–Re bonding is for clusters at the valley sites.

4 Conclusions

These experiments demonstrate (a) preferential nucleation of cobalt nanoclusters within the valleys of the faceted surface, and (b) the ability to vary the size of the nanoclusters by varying the facet size, cobalt coverage, and annealing temperature. The observation that metallic

nanoclusters can be grown at specific sites with a relatively narrow size distribution by a self assembly technique (vapor deposition onto an oxidized nanotemplate substrate) may have broad implications in the search for increased selectivity in model catalytic studies.

Acknowledgments This work was supported by the US Department of Energy, Office of Basic Energy Sciences.

References

1. Somorjai GA, Borodko YG (2001) *Catal Lett* 76:1
2. Somorjai GA, York RL, Butcher D, Park JY (2007) *Phys Chem Chem Phys* 9:3500
3. Chini P (1980) *J Organomet Chem* 200:37
4. Cox DM, Kaldor A, Fayet P, Eberhardt W, Brickman R, Sherwood RF, Sondericher ZD (1990) *ACS Symp Ser* 437:172
5. Leskiw BD, Castleman AW (2000) *Chem Phys Lett* 316:31
6. Trevor DJ, Cox DM, Kaldor A (1990) *J Am Chem Soc* 112:3742
7. Abbet S, Sanchez A, Heiz U, Schneider W-D, Ferrari AM, Pacchioni G, Rosch N (2000) *Surf Sci* 454–456:984
8. Campbell CT (1997) *Surf Sci Rep* 27:1
9. Goodman DW (2003) *J Catal* 216:213
10. Engelmann GE, Ziegler JC, Kolb DM (1998) *Surf Sci* 401:L420
11. Gunter PLJ, Niemantsverdriet JW, Ribeiro FH, Somorjai GA, York RL, Butcher D, Park JY (1997) *Catal Rev Sci Eng* 39:77
12. Heiz U, Sanchez A, Abbet S, Schneider W-D (1999) *Eur Phys J D* 9:35
13. Lee H, Habas SE, Kweskin S, Butcher D, Somorjai GA, Yang P (2006) *Angew Chem Int Ed* 45:7824
14. Ono LK, Roldan-Cuenya B (2007) *Catal Lett* 113:86
15. Shevchenko EV, Talapin DV, Kotov NA, O'Brien S, Murray CB (2006) *Nature* 439:55
16. Wang H, Chen W, Madey TE (2006) *Phys Rev B* 74:205426
17. Szczepkiewicz A, Ciszewski A, Bryl R, Oleksy C, Nien C-H, Wu Q, Madey TE (2005) *Surf Sci* 599:55
18. Nien C-H, Madey TE (1999) *Surf Sci* 433–435:254
19. Bowker MK, Bowker LJ, Bennett RA, Stone P, Ramirez-Cuesta A (2000) *J Mol Catal A: Chem* 163:221
20. Fujikawa K, Suzuki S, Koike Y, Chun W-J, Asakura K (2006) *Surf Sci* 600:L117
21. Zhou J, Chen DA (2003) *Surf Sci* 527:183
22. Baumer M, Freund H-J (1999) *Prog Surf Sci* 61:127
23. Lehnert A, Krupski A, Degen S, Franke K, Decker R, Rusponi S, Kralj M, Becker C, Brune H, Wandelt K (2006) *Surf Sci* 600:1804
24. Rose V, Podgursky V, David R, Franchy R (2007) *Surf Sci* 601:786
25. Sedona F, Agnoli S, Fanetti M, Kholmanov I, Cavaliere E, Gavioli L, Granozzi G (2007) *J Phys Chem C* 111:8024
26. Revenant C, Leroy F, Renaud G, Lazzari R, Létoublon A, Madey T (2007) *Surf Sci* 601:3431